

## RESEARCH ARTICLE



# Overexpression of ST8Sia1 inhibits tumor progression by TGF- $\beta$ 1 signaling in rectal adenocarcinoma and promotes the tumoricidal effects of CD8<sup>+</sup> T cells by granzyme B and perforin

Chang Zhang<sup>a\*</sup>, Yeli Wang<sup>a\*</sup>, Yao Yu<sup>b\*</sup>, Yanchao Pang<sup>a\*</sup>, Xiao Xiao<sup>c</sup> and Leilei Hao<sup>a</sup> 

<sup>a</sup>Department of Anorectal, The Affiliated Yantai Yuhuangding Hospital of Qingdao University, Yantai City, Shandong Province, China;

<sup>b</sup>Department of General Pediatric Surgery, The Affiliated Yantai Yuhuangding Hospital of Qingdao University, Yantai City, Shandong Province, China; <sup>c</sup>Department of Neurology, The Affiliated Yantai Yuhuangding Hospital of Qingdao University, Yantai City, Shandong Province, China

## ABSTRACT

**Background:** Rectal adenocarcinoma (READ) involves the dysregulated expression of alpha 2,8-Sialyltransferase1 (ST8Sia1) although its role during READ's progression is unclear.

**Methods:** The mRNA level of ST8Sia1 was analyzed based on The Cancer Genome Atlas (TCGA), Gene Expression Omnibus (GEO), and Tumor Immune Estimation Resource (TIMER) 2.0. Furthermore, the prognostic and significance of ST8Sia1 in READ was assessed through Kaplan-Meier curve, univariate, multivariate Cox regression, and receiver operating characteristic (ROC) methods. The role of ST8Sia1 in the READ immune microenvironment was explored using ESTIMATE analysis and TIMER databases. Furthermore, the expression of ST8Sia1 in tissues was analyzed using real-time quantitative polymerase chain reaction (RT-qPCR), western blotting (WB), and immunohistochemistry (IHC). Perforin and Granzyme B secretion by CD8<sup>+</sup> T cells, as well as tumor cell apoptosis, were detected after co-culturing CD8<sup>+</sup> T cells with READ tumor cells and ST8Sia1-overexpression (ST8Sia1-OE) tumor cells. Furthermore, we examined the interaction between ST8Sia1 and TGF- $\beta$ 1 in READ cells.

**Results:** ST8Sia1 exhibited excellent diagnostic capability for READ, with positive correlations to immune response and negative correlations to tumor purity. Increased levels of perforin and Granzyme B from CD8<sup>+</sup> T cells were observed in vitro, enhancing tumor cell apoptosis. ST8Sia1 interacts with TGF- $\beta$ 1, mediating its inhibitory effects on READ development.

**Conclusions:** ST8Sia1 is a potential diagnostic biomarker and therapeutic target for READ, enhancing CD8<sup>+</sup> T cell function and possibly improving patient outcomes through cellular immunotherapy.

**Abbreviations:** BPs: (biological processes); CCs: (cellular components); COAD: (colon adenocarcinoma); ESTIMATE: (Estimation of Stromal and Immune cells in Malignant Tumor tissues using Expression data); GEO: (Gene Expression Omnibus); GO: (Gene Ontology); GSEA: (Gene Set Enrichment Analysis); GSVA: (Gene Set Variation Analysis); HCK: (hemopoietic cell kinase); HNSC: (head and neck squamous cell carcinoma); ICPs: (Immune checkpoints); IHC: (Immunohistochemistry); KEGG: (Kyoto Encyclopedia of Genes and Genomes); LCK: (lymphocyte-specific kinase); LUSC: (lung squamous cell carcinoma); MHC-I/-II: (major histocompatibility complex-I/-II); MFs: (molecular functions); READ: (Rectal adenocarcinoma); ROC: (receiver operating characteristic); GalNTs: (GalNAc transferases); OS: (overall survival); RT-qPCR: (Real-time quantitative PCR); FUT: (fucosyltransferase); STs: (Sialyltransferases); ST8Sias: (alpha2,8-Sialyltransferases); ST8Sia1-OE: (ST8Sia1 overexpression); STAT1: (signal transducer and activator of transcription 1); TCGA: (The Cancer Genome Atlas); TIMER 2.0: (Tumor Immune Estimation Resource 2.0); TME: (tumor microenvironment); FBS: (Fetal Bovine Serum)

## ARTICLE HISTORY

Received 9 February 2024

Revised 23 May 2024


Accepted 29 October 2024

## KEYWORDS

Sialyltransferase; ST8Sia1; rectal adenocarcinoma; CD8<sup>+</sup> T-cell; immune microenvironment

**CONTACT** Leilei Hao  [2016172021@mail.sdu.edu.cn](mailto:2016172021@mail.sdu.edu.cn)  Department of Anorectal, The Affiliated Yantai Yuhuangding Hospital of Qingdao University, No. 20 Yudong Road, Zhifu District, Yantai City 264001, Shandong Province, China; Xiao Xiao  [researchxx@sina.com](mailto:researchxx@sina.com)  Department of Neurology, The Affiliated Yantai Yuhuangding Hospital of Qingdao University, No. 20 Yudong Road, Zhifu District, Yantai City 264001, Shandong Province, China.

\*These authors contributed equally to this work.

 Supplemental data for this article can be accessed online at <https://doi.org/10.1080/07853890.2024.2439539>.

© 2025 The Author(s). Published by Informa UK Limited, trading as Taylor & Francis Group

This is an Open Access article distributed under the terms of the Creative Commons Attribution-NonCommercial License (<http://creativecommons.org/licenses/by-nc/4.0/>), which permits unrestricted non-commercial use, distribution, and reproduction in any medium, provided the original work is properly cited. The terms on which this article has been published allow the posting of the Accepted Manuscript in a repository by the author(s) or with their consent.

## Introduction

Rectal adenocarcinoma (READ) is a common gastrointestinal tumor malignancy, with a 5-year survival rate of over 90% for patients in the early stage, but less than 50% in patients in the late stage [1]. Numerous factors are related to the etiology of READ, including environmental factors, dietary habits, and genetic factors [2]. Moreover, as the most common subtype among Asians, READ has increased in the past decade and has been a formidable challenge in China [3, 4]. Currently, clinicians use surgical resection and chemotherapy as the main approaches to decrease the risk of distant metastasis and improve the overall survival (OS) of patients with READ [5]. However, surgical resection and chemotherapy may have adverse effects on the human body, such as affecting anorectal function [6]. Overall, identifying biomarkers is crucial for diagnosing pathological features and improving patient prognosis.

Glycosylation is an enzymatic process that forms or removes glycosidic linkages between glycans and other glycans, proteins, and lipids with glycosyltransferases or glycosidases [7]. Glycosylation regulates the localization, function, and activity of proteins in tissues and cells, affecting various important biological activities, such as cell recognition, differentiation, signal transduction, and immune response. Abnormal glycosylation is associated with differential expression of glycosyltransferases and glycosidases in cancer [8]. The aberrant expression of sialyltransferases (STs), which are responsible for the addition of sialic acid to glycoconjugates, regulates tumorigenesis and immune evasion [9–11]. ST8-sialyltransferases (ST8Sias), including ST8Sia1, ST8Sia2, ST8Sia3, ST8Sia4, ST8Sia5, and ST8Sia6, transfer Neu5Ac residues to complex glycans *via*  $\alpha$ -2,8-linkage [12]. Increasing evidence has indicated that ST8Sias are associated with various cancers. Previous reports have demonstrated that ST8Sia1 is overexpressed in melanoma, glioblastoma, and estrogen receptor-negative breast cancer [13–15]. Additionally, ST8Sia2 promotes invasiveness and sensitivity to chemotherapy in hepatocellular carcinoma [16]. ST8Sia4 inhibits the occurrence of follicular thyroid carcinoma [17]. In contrast, highly metastatic breast cancer cells demonstrated higher ST8Sia4 levels, and knockdown of ST8Sia4 significantly inhibited malignant behavior [18]. Low ST8Sia6 expression promotes colon cancer progression [19]. However, the occurrence and development of abnormal ST8Sia1 expression remains unclear.

This study revealed downregulated ST8Sia1 mRNA levels in the READ tissues and promoter methylation levels of ST8Sia1 were upregulated. We revealed the molecular functions and underlying immune regulatory

mechanisms of ST8Sia1 in READ using gene set variation analysis (GSVA), Kyoto Encyclopedia of Genes and Genomes (KEGG), and Gene Ontology (GO) enrichment analyses. Upregulated ST8Sia1 may inhibit tumor migration, invasion, and proliferation. Increased perforin and Granzyme B secretion by CD8<sup>+</sup> T cells was detected when ST8Sia1 overexpressing (ST8Sia1-OE) tumor cells were cocultured *in vitro*, causing a higher rate of tumor cell apoptosis. Moreover, the presence of TGF- $\beta$ 1 is crucial for restraining the incidence and progression of READ both *in vivo* and *in vitro* in the context of ST8Sia1-OE.

## Materials and methods

### Data sources and preprocessing

The Cancer Genome Atlas (TCGA)-READ mRNA expression profiles with intact clinical information were downloaded from TCGA database. The TCGA-READ dataset contained 163 primary tumors and 10 normal samples. [Supplementary Table 1](#) lists the detailed information. The GSE87211 dataset was downloaded from the Gene Expression Omnibus (GEO) database, which recorded the gene expression profiling data of 203 READ tumor tissue samples and 160 normal samples (GPL13497 platform) [20]. The R package “DESeq2” or “Limma” was used for ST8Sia1 expression analysis. Additionally, ST8Sia1 expression in various cancer types was investigated using the Tumor Immune Estimation Resource 2.0 (TIMER 2.0) database [21].

### Promoter methylation analysis

The UALCAN database [22] was used to explore the correlation between the promoter methylation levels of ST8Sia1 and their different stages in patients with READ. The analysis was conducted by entering ST8Sia1 symbols with the TCGA dataset “READ” and choosing the “Methylation” in the “Links for analysis” module.

### ESTIMATE analysis

ESTIMATE method [23] was used to evaluate the degrees of immune cells infiltration (ImmuneScore), the stromal content (StromalScore), the stromal-immune comprehensive score (ESTIMATEScore), and tumor purity for each READ sample by “estimate” package in R environment.

### Immune infiltration analysis

The TIMER online database was used to explore the correlation between ST8Sia1 expression and related

immune cell infiltration in READ. The “Gene” module was used to analyze and visualize associations between ST8Sia1 expression and the abundance of 6 tumor-infiltrating immune cell subtypes (B cells, CD4<sup>+</sup> T cells, CD8<sup>+</sup> T cells, macrophages, neutrophils, and dendritic cells). The association of immune cell markers and ST8Sia1 expression was evaluated with the “Correlation” module in the TIMER database.

### GSVA

The list of GO terms for immune processes was obtained from the Gene Set Enrichment Analysis (GSEA) web portal. The “GSVA” package in R was used to calculate the functional enrichment score of each READ sample [24]. The results were then drawn using the “pheatmap” package or “corrgram” package in the R environment.

### Gene functional enrichment analysis

The most relevant genes of ST8Sia1 were respectively uploaded to the Database for Annotation, Visualization, and Integrated Discovery (DAVID 6.8) [25, 26]. GO analysis, including BPs, CCs, molecular function (MFs), and KEGG enrichment results, were obtained. Finally, the enrichment results were drawn by the “ggplot2” in R.

### Real-time quantitative polymerase chain reaction (RT-qPCR)

TRIzol reagent was used to extract total RNA from tissues. The Bio-Rad iScript cDNA synthesis kit was used for the reverse transcription of RNA to cDNA. Differential mRNA expression was determined using a CFX Connect™ Real-time system (Bio-Rad, United States) following the manufacturer’s instructions (Applied Biosystems). The RT-qPCR results were analyzed using the  $2^{-\Delta\Delta C_t}$  method. GAPDH was used as the standard control. [Supplementary Table 2](#) lists the specific primers used.

### Immunoprecipitation and WB

Overnight incubation with gentle shaking at 4°C was performed using the indicated antibodies (5 µl) and the protein lysate (1000 µg). Following this, a mixture of 30 µl protein G-sepharose (Beytine, China) was added and rotated for 4h at 4°C. The beads were then subjected to three washes with protein lysis buffer, and the bound proteins were either boiled for 5 min in 25 µl of 2×Laemmli sample buffer or eluted using

Tris-HCl buffer (pH = 2.5). Protein lysates were extracted, loaded onto the SDS polyacrylamide gels, and subjected to electrophoresis. Proteins were transferred to a nitrocellulose membrane after electrophoresis. Then, the nitrocellulose membranes were incubated with primary antibodies at 4°C overnight. the nitrocellulose membranes were incubated with secondary antibodies at 37°C for 1h after washing with TBST. An iBright CL1000 imaging system (Thermo Fisher) was used to capture the images. Specific primary antibodies used are listed in [Table 1](#).

### In vivo tumor growth assay

All athymic BALB/c male nude mice (4–6 weeks old) were purchased from Shulaibao Biotech (Wuhan, China) and maintained at constant temperature (23–25°C) with controlled light/dark cycles (12h/12h) at The Affiliated Yantai Yuhuangding Hospital of Qingdao University. A total of 1×10<sup>7</sup> Control, ST8Sia1-OE and ST8Sia1-OE-shTGF-β1 HCT15 cells were mixed with 150 µL PBS buffer and injected into male nude mice. Tumor growth was measured weekly. The mice were sacrificed using 60% carbon dioxide after 28 days of the experiment. Tumor volumes were calculated using the following formula: tumor volume = (length) × (width)<sup>2</sup> × 0.5, and the weights of the tumors were recorded. All animal experiments were approved by the Ethics Committee of the Affiliated Yantai Yuhuangding Hospital of Qingdao University (2022YHDYY-16). All investigations adhered to ARRIVE and institutional protocols.

### Hematoxylin-eosin (HE) and immunohistochemistry (IHC) analysis

There were 10 samples of READ tissues (*n*=5) and para-cancerous tissues (*n*=5) from The Affiliated Yantai Yuhuangding Hospital of Qingdao University, which were included in the tissue collection. The study was conducted in accordance with the Declaration of Helsinki (as revised in 2013). The study was approved

**Table 1.** The list of specific primary antibodies.

Antibody	Band	Category number	Dilution rate with TBST
ST8Sia1	Proteintech	24918-1-AP	1:1000
Bcl-2	Cell Signaling Technology	#3498	1:1000
Bax	Proteintech	50599-2-Ig	1:1000
Cleaved caspase 3	Proteintech	25128-1-AP	1:1000
PARP1	Cell Signaling Technology	#5625	1:1000
GAPDH	Proteintech	60004-1-Ig	1:5000

by Institutional Review Board of The Affiliated Yantai Yuhuangding Hospital of Qingdao University (No.2022YHRTL223). Before the study, we obtained the written informed consent of all participants or legal guardians to ensure that they have a comprehensive understanding of the purpose, procedures, potential risks and benefits of the study. HE staining was performed on 4- $\mu$ m-thick sections of mouse tumor tissue from different groups. The staining process lasted for 1 min and the sections were subsequently differentiated in acidic alcohol for 30s. The sections were dehydrated in 95% ethanol for 50s, cleared in xylene, and mounted. For IHC, the tissues of patients with READ and mouse tumor tissues from different groups were fixed with 4% paraformaldehyde, permeabilized with 0.5% Triton X-100 in PBS for 15 min, and blocked with 3% bovine serum albumin. Then, the tissues were incubated overnight at 4°C with primary antibodies (1:100). This study used antibodies similar to the WB. Images were obtained using a microscope (Leica, Germany). These average values of immune reactivity were divided into five scoring groups: 1, not detected; 2, <10% positive cells; 3, 10-20% weak to moderately positive cells; 4, 10-20% strong positive cells or 20-50% weak positive cells; 5, 20-50% positive cells with moderate to significant reactivity or >50% positive cells.

### **Cell culture and transfection**

HCT-116 (CCL-247), HCT-15 (CCL-225), and FHC (CRL-1831) cells were purchased from ATCC (USA) and cultured in McCoy's 5A or RPMI-1640 medium supplemented with 10% Fetal Bovine Serum (FBS) and 1% penicillin/streptomycin. Cells were incubated in 5% CO<sub>2</sub> at 37°C. CD8<sup>+</sup> T cells were derived from the human peripheral blood. Briefly, peripheral blood from healthy volunteers was extracted using a disposable sterile syringe, followed by red blood cell lysis. Immune magnetic beads (Becton, Dickinson and Company, USA) were used for separation to obtain CD8<sup>+</sup> T cells, which were then co-cultured with HCT-116 or HCT-15 cells. HCT-116 or HCT-15 cells ( $1 \times 10^5$ /well) were seeded in a 6-well plate on the previous day, and purified CD8<sup>+</sup> T cells ( $5 \times 10^5$ /well) were seeded in the upper chamber of the transwell chamber. ST8Sia1-OE and control plasmids were constructed (ABM, Nanjing, China). The lipo3000 reagent (Invitrogen, USA) was used to transfect cells following the manufacturer's protocol. Puromycin (Beyotime, China) was used for drug screening after incubating the cells for 48h, and the efficiency of ST8Sia1-OE was measured by RT-qPCR and WB. The co-culture system was maintained for 48-72h and further analyzed. The CD8<sup>+</sup> T cells located

in the upper chamber of the transwell system were harvested for perforin and granzyme B analysis, while the HCT-116 or HCT-15 cells situated in the lower chamber were collected to assess apoptosis.

### **Enzyme-linked immunosorbent assay (ELISA)**

The TGF- $\beta$ 1 content in the culture medium of co-cultured CD8<sup>+</sup> T cells and READ cells was measured using a TGF- $\beta$ 1 ELISA Kit (E-EL-0162, Elabscience, Wuhan, China). According to the instructions provided in the experimental manual. In brief, TGF- $\beta$ 1 in the sample binds to the pre-coated anti-TGF- $\beta$ 1 antibody on the ELISA plate, and the free components were washed away. Biotinylated anti-TGF- $\beta$ 1 antibody and horseradish peroxidase-conjugated avidin were then added. The anti-TGF- $\beta$ 1 antibody binds to TGF- $\beta$ 1 bound to the coated antibody, and biotin specifically binds to avidin to form an immunocomplex. The free components were washed away. Substrate (TMB) was added, which turned blue under the catalysis of horseradish peroxidase. After the stop solution was added, the color turned yellow. The OD value was measured at 450nm using an enzyme immunoassay analyzer, and TGF- $\beta$ 1 concentration was proportional to the OD450 value. The TGF- $\beta$ 1 concentration in the samples was calculated by plotting a standard curve. Cell culture supernatants from co-cultured CD8<sup>+</sup> T cells and READ cells were collected after 72h, and analyzed for the presence of IFN- $\gamma$  using an ELISA kit according to the manufacturer's instructions (R&D Systems).

### **Cell invasion assay**

Approximately  $5 \times 10^4$  HCT-116 and HCT-15 cells, transfected with either the ST8Sia1-OE or the control plasmid, were placed into the upper chamber (Corning, USA) with 40  $\mu$ l of Matrigel in a 24-well transwell chamber. The cells were cultured in 200  $\mu$ l of medium without FBS. A medium containing 10% FBS was added to the lower chamber. The cells were fixed with a solution of 4% paraformaldehyde after a 48-h incubation period. Cells that invaded the surface of the chamber were stained with 1% crystal violet and washed with water. After drying, the chamber was counted under a high-magnification microscope (Leica, Germany).

### **Wound healing assay**

A wound healing assay was performed to evaluate cell migration. Briefly, cells ( $7 \times 10^5$ /well) were seeded in a



6-well plate and allowed to form a confluent monolayer. Subsequently, a wound was created by scratching with a 200- $\mu$ l of a pipette tip and photographed immediately with a microscope at 100 $\times$  magnification. The same regions were subsequently imaged following an incubation period of 24h in medium containing 2% FBS.

### **5-ethynyl-2'-deoxyuridine (EdU) and reactive oxygen species (ROS) assay**

EdU, a nucleoside analog of thymidine, is involved in DNA synthesis. Cell proliferation and cell cycle distribution were measured. Cells were plated at a density of  $2.5 \times 10^5$ /well in a 6-well plate with 5% CO<sub>2</sub> at 37°C. Cells were incubated with EdU or ROS staining kit (Beyotime, Shanghai, China) for 48h following the manual with 2h for immunofluorescence staining. DAPI was used to stain the cell nuclei for 5min, and fluorescence was observed under a microscope. The percentage of EdU- and ROS-positive cells was calculated.

### **Colony forming assay**

Approximately  $1 \times 10^3$  cells were seeded in 6-well plates. After 14days of culture, the cells were fixed with 4% paraformaldehyde for 30min and then stained with 1% crystal violet for 30min. The cell clusters comprised more than 50 cells and were counted using the ImageJ software (version 4.0).

### **Flow cytometry assay**

The identification of apoptosis in cells was conducted using the Annexin V-FITC Apoptosis Detection kit and following the manufacturer's recommended analysis protocol (BD Pharmingen, USA) to detect tumor cell apoptosis after co-culture of CD8<sup>+</sup> T cells ( $5 \times 10^5$ /well) and HCT-116 or HCT-15 cells ( $1 \times 10^5$ /well) for 48-72h. Additionally, CD8<sup>+</sup> T cells were harvested and stained for flow cytometric analysis. Cells were suspended in 100 $\mu$ l of cold PBS containing appropriate concentrations of Granzyme B and Perforin (Cell Signaling Technology, USA) and incubated in the dark at 37°C for 60min. The cells were resuspended in PBS and analyzed on a BD Accuri™ C6+ flow cytometer, and FlowJo software was used to analyze the data.

### **Ethical considerations**

The authors are accountable for all aspects of the work in ensuring that questions related to the accuracy or

integrity of any part of the work are appropriately investigated and resolved. The study was conducted in accordance with the Declaration of Helsinki (as revised in 2013). The study was approved by Institutional Review Board of The Affiliated Yantai Yuhuangding Hospital of Qingdao University (No.2022YHRTLL223). Before the study, we obtained the written informed consent of all participants or legal guardians to ensure that they have a comprehensive understanding of the purpose, procedures, potential risks and benefits of the study. All animal experiments were approved by the Ethics Committee of the Affiliated Yantai Yuhuangding Hospital of Qingdao University (2022YHDYY-16). All investigations adhered to ARRIVE and institutional protocols.

### **Statistical analysis**

Statistical analyses and visualizations were performed using R 4.1.3, Statistical Product Service Solutions (SPSS 26.0), GraphPad Prism 8.0, and ImageJ software v.4.0. Student's t-test was used for comparisons between the two groups. Statistical significance was set at  $p < 0.05$ .

## **Results**

### **ST8Sia1 is significantly reduced in tumor tissues of READ**

Utilizing the RNA sequencing profiles derived from TCGA and GEO RNA-seq datasets, we analyzed READ tumor tissues from afflicted patients alongside non-tumor tissue specimens from healthy controls. A significant reduction in ST8Sia1 mRNA levels was observed in READ tissues (Figure 1A). Additionally, we assessed the expression of ST8Sia1 across various stages of READ and found a decrease in expression correlating with the progressive stages of READ. Additionally, the expression of ST8sia1 was lower than normal at the four different stages of READ (Figure 1B). Moreover, a notable decrease in ST8Sia1 mRNA levels was confirmed in READ tissues in the GSE87211 dataset (Figure 1C).

In a subsequent analysis, ST8Sia1 mRNA levels were found to be significantly lower in READ tumor tissues as sourced from GEPIA and TIMER 2.0, underscoring the potential pivotal roles of ST8Sia1 in tumorigenesis (Figure 1D and E). Our findings were further corroborated by an additional validation of ST8Sia1 expression in patients with READ, in which a significant reduction in ST8Sia1 mRNA expression was observed in the tumor tissues of these patients (Figure 1F). Complementarily,

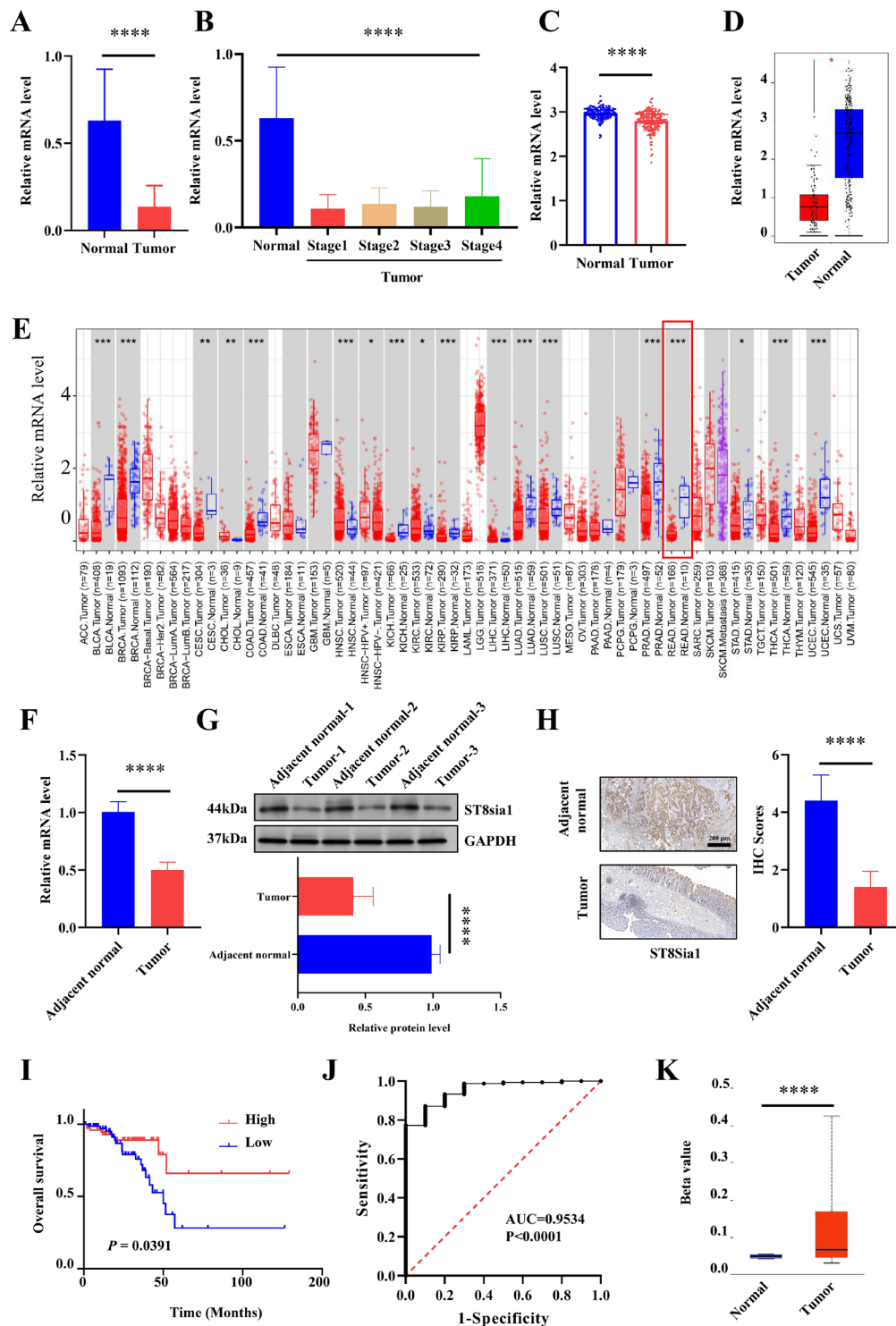


**Figure 1.** The down-regulated ST8Sia1 expression in patients with READ. (A) Comparison of ST8Sia1 transcriptional levels between tumor tissues ( $N=163$ ) from READ and non-tumor tissues ( $N=10$ ) from healthy control by Student's t-test based on TCGA-READ databases. (B) Correlations between the ST8Sia1 expression and the main pathological stages, including stage 1 ( $N=28$ ), stage 2 ( $N=51$ ), stage 3 ( $N=51$ ), and stage 4 ( $N=23$ ) of were investigated based on the TCGA database. (C) The mRNA expression levels of ST8Sia1 in READ tumor tissues ( $N=203$ ) and normal tissues ( $N=160$ ) in the GEO database (GSE87211). (D) ST8Sia1 expression in tumor tissues of READ patients and normal tissues from the TCGA database analyzed by the GEPIA database. (E) ST8Sia1 expression in different types of tumor tissues and normal tissues from the TCGA database analyzed by the TIMER 2.0 database. The red and blue boxes represent tumor tissues and normal tissues, respectively. The purple box represents metastasis tumor. The ST8Sia1 level was detected in tumor tissues and adjacent normal tissues of patients with READ by RT-qPCR (F) and WB analysis (G) ( $n=3$ ). GAPDH served as a control. (H) Representative picture of ST8Sia1 was detected in tumor tissues and adjacent normal tissues of patients with READ by IHC ( $n=3$ ). Scale bars = 200  $\mu$ m. (I) Kaplan-Meier curve was used to evaluate the prognostic risk of ST8Sia1 gene. (J) ROC curve analysis of the diagnostic value of ST8Sias for READ. (K) DNA methylation level of ST8Sia1 gene in patients with READ were higher than in normal tissues. P-values of <0.05 were considered statistically significant, \* $p$ <0.05, \*\* $p$ <0.01, \*\*\* $p$ <0.001, and \*\*\*\* $p$ <0.0001.

the results of WB and IHC analyses were consistent with those of RT-qPCR, confirming the consistency of our research findings. (Figure 1G and H). Furthermore, we investigated the association between ST8Sia1 expression and prognosis using the Kaplan-Meier (K-M) curve. Remarkably, patients with READ exhibiting higher levels of ST8Sia1 were associated with improved Overall Survival (OS) compared to those with lower ST8Sia1 levels (Figure 1I). The ROC curve demonstrated a compelling AUC value of 0.9534 for ST8Sia1 expression (Figure 1J). Intriguingly, an upregulation in the DNA methylation of ST8Sia1 was identified in READ, in contrast to the downregulated expression of the ST8Sia1 gene (Figure 1K and Supplementary Figure 1). In addition, the upregulation of DNA methylation of ST8Sia1 in four different stages of tumors in READ varies, especially in the second and fourth stages, and the upregulation of DNA methylation of ST8Sia1 is more pronounced.

### ***The ST8Sia1 gene may regulate immune response in READ***

In our study, genes most closely related to ST8Sia1 were selected from the TCGA-READ database, followed by functional enrichment analysis conducted using the DAVID 6.8 database. The Biological Processes (BPs) predominantly associated with ST8Sia1 encompass immune response, inflammatory response, signal transduction, cell migration, and cell adhesion (Figure 2A). These genes were significantly correlated with the plasma membrane within Cellular Components (CCs) (Figure 2B). Furthermore, ST8Sia1 was associated with extracellular matrix structural constituents, heparin binding, and transmembrane signaling receptor activity (Figure 2C). Remarkably, these genes were mainly enriched in cell adhesion molecules and selected signaling pathways (PI3K-Akt and Rap1 signaling pathways) as identified by KEGG analysis (Figure 2D).

We delved deeper into the effect of ST8Sia1 on immune regulation. The level of ST8Sia1 showed a positive association with numerous immune functions, including immune response regulation and T/B cell activation involved in the immune response (Figure 2E). We further investigated the role of ST8Sia1 in immune cell infiltration in READ. Notably, the ST8Sia1 level was significantly correlated with the abundance of infiltrating immune cells in READ and inversely correlated with tumor purity in READ (Figure 2F).

In a subsequent analysis, the correlation between ST8Sia1 expression and immune cell markers was examined using TIMER 2.0. Almost all immune cell markers were correlated with the ST8Sia1 gene (Table 2).

The expression of CD8<sup>+</sup> and CD4<sup>+</sup> T cells was downregulated in READ tissues compared to adjacent normal tissues, as determined by IHC (Figure 2G and H). Collectively, our findings underscore the probable pivotal role of ST8Sia1 in modulating immune responses and in contributing to tumorigenesis in READ.

### ***The ST8Sia1 gene may predict the immunotherapy response of READ***

We investigated the association between ST8Sia1 levels and four types of ESTIMATE scores to elucidate the role of ST8Sia1 in the tumor microenvironment (TME) of READ. A strong positive correlation was observed between ST8Sia1 levels and stromal score, immune score, and ESTIMATEScore in READ (Figure 3A–C). Conversely, ST8Sia1 levels were negatively correlated with tumor purity (Figure 3D). These findings suggest that downregulation of ST8Sia1 may contribute to an immunosuppressive state in READ. The correlations between ST8Sia1 and these seven metagenes were illustrated using corrgrams (Figure 3E), where ST8Sia1 showed a positive correlation with HCK, interferon, LCK, MHC-II, and STAT1 metagenes. Subsequently, we validated the correlations between ST8Sia1 and multiple immune checkpoint proteins (ICPs) in READ samples to explore the potential implications of ST8Sia1 in immunotherapy, utilizing TIMER 2.0. Our analysis revealed a prominent positive association between ST8Sia1 and most ICPs (Figure 3F). Furthermore, we assessed the relationship between ST8Sia1 and immune function by calculating correlations with seven inflammatory activity-related metagene clusters encompassing 104 genes (Supplementary Table 3). These clusters include HCK, IgG, interferon, LCK, MHC-I/-II, and STAT1 [27, 28]. Collectively, our data suggest that ST8Sia1 may serve as a predictive marker for immunotherapy response in patients with READ.

### ***ST8Sia1-OE inhibited the biological function of READ cells***

Compared with FHC cells, a normal human colorectal epithelial cell, HCT-15 and HCT-116 cells showed significantly lower expression of ST8Sia1 (Supplementary Figure 2). Therefore, we engineered elevated expression of ST8Sia1 in HCT-15 and HCT-116 cells to elucidate the functional role of ST8Sia1 in READ cells. Both protein and transcriptional levels of ST8Sia1 were markedly augmented in ST8Sia1-OE cells (Figure 4A–C). EdU and colony-forming assays demonstrated a reduction in tumor cell proliferation with increased ST8Sia1 expression (Figure 4D–E and G). Furthermore, ST8Sia1-OE

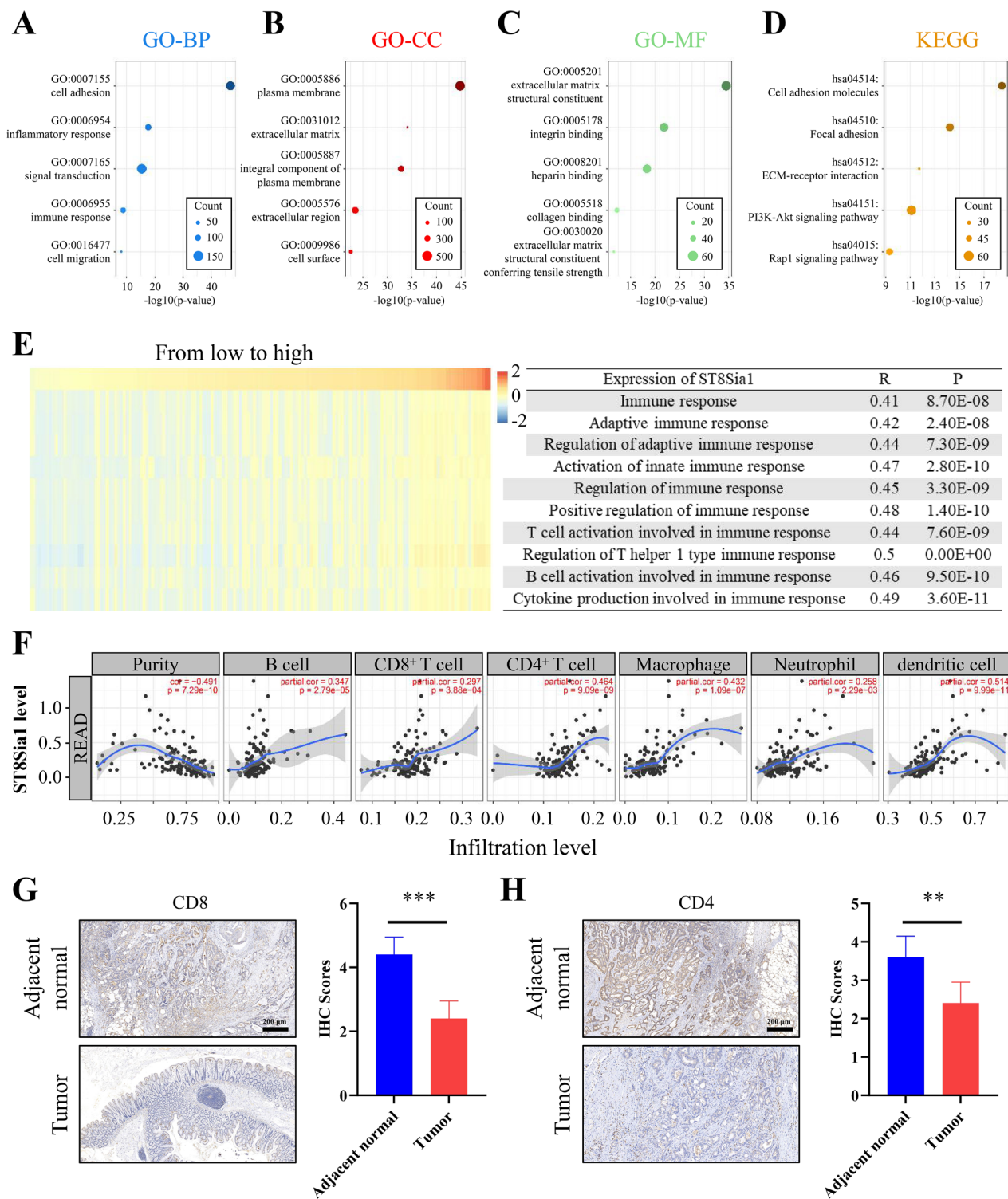


**Figure 2.** The ST8Sia1 gene may regulate immune response in READ. (A-D) GO and KEGG pathway enrichment analysis of the most associated 1372 genes of ST8Sia1 using DAVID 6.8 and the “ggplot2” in R. The size of the point indicated the count of genes in the pathway and the color depth indicated the degree of statistical significance. The deeper the color of the point represented the more statistically significant the corresponding pathway. (E) The heatmap revealed the expression of ST8Sia1 and the enrichment scores of the immune functions of each patient from the TCGA database. The specific correlation coefficients and P-value were shown on the right. (F) The relationship between the ST8Sia1 expression and the infiltration degree of six types of immune cells in READ via TIMER 2.0 database. The representative picture of CD8 (G) and CD4 (H) was detected in tumor tissues and the normal group of patients with READ by IHC ( $n=3$ ). Scale bars = 200  $\mu\text{m}$ . P-values of  $<0.05$  were considered statistically significant, \*\* $p<0.01$  and \*\*\* $p<0.001$ .



**Table 2.** The *ST8Sia1* expression was significantly correlated with the infiltration levels of various immune cell markers based on TIMER 2.0 database.

Gene Name	Gene Marker	Corelation	P-value
CD8 <sup>+</sup> T cell	<i>CD8A</i>	0.45	1.21E-09
T cell	<i>CD8B</i>	0.308	5.43E-05
	<i>CD3D</i>	0.417	2.33E-08
	<i>CD3E</i>	0.475	9.84E-11
	<i>CD2</i>	0.562	3.14E-15
B cell	<i>CD19</i>	0.282	2.36E-04
	<i>CD79A</i>	0.362	1.66E-06
Natural killer cell	<i>KIR2DL1</i>	0.178	2.21E-02
	<i>KIR2DL3</i>	0.157	4.31E-02
	<i>KIR3DL1</i>	0.196	1.14E-02
	<i>KIR3DL3</i>	0.085	2.74E-01
Neutrophil	<i>NCAM1</i>	0.566	1.97E-15
	<i>ITGAM(CD11b)</i>	0.586	1.07E-16
	<i>CEACAM8(CD66b)</i>	-0.221	4.16E-03
	<i>CCR7</i>	0.395	1.36E-07
Type 1 T helper cell	<i>CD59</i>	0.507	3.30E-12
	<i>TBX21</i>	0.433	5.44E-09
	<i>STAT4</i>	0.546	2.75E-14
	<i>STAT1</i>	0.538	7.42E-14
Type 2 T helper cell	<i>IFNG (IFN-γ)</i>	0.344	5.71E-06
	<i>TNF-α (TNF)</i>	0.48	6.02E-11
	<i>STAT5A</i>	0.282	2.36E-04
	<i>IL13</i>	0.293	1.29E-04
Type 17 T helper cell	<i>GATA3</i>	0.49	2.18E-11
	<i>STAT6</i>	0.099	2.06E-01
	<i>CCR4</i>	0.533	1.38E-13
	<i>STAT3</i>	0.407	5.17E-08
T follicular helper cell	<i>IL17A</i>	-0.141	7.06E-02
	<i>IL21</i>	0.104	1.83E-01
Tumor associated macrophages	<i>BCL6</i>	0.406	5.60E-08
	<i>CCL2</i>	0.68	6.92E-24
Dendritic cell	<i>IL10</i>	0.432	6.23E-09
	<i>CD68</i>	0.389	2.27E-07
	<i>CD1C(BDCA-1)</i>	0.513	1.54E-12
	<i>NRP1(BDCA-4)</i>	0.703	5.07E-26
Regulatory T cell	<i>HLA-DPB1</i>	0.571	9.83E-16
	<i>HLA-DQB1</i>	0.351	3.47E-06
	<i>HLA-DPA1</i>	0.609	3.09E-18
	<i>HLA-DRA</i>	0.547	2.60E-14
Monocyte	<i>ITGAX(CD11c)</i>	0.593	4.06E-17
	<i>FOXP3</i>	0.601	1.06E-17
	<i>STAT5B</i>	0.512	1.72E-12
	<i>TGF-β1(TGFβ1)</i>	0.522	5.34E-13
M1 macrophage	<i>CD86</i>	0.646	5.11E-21
	<i>CSF1R(CD115)</i>	0.604	6.83E-18
M2 macrophage	<i>NOS2</i>	-0.123	1.15E-01
	<i>PTGS2(COX2)</i>	0.292	1.33E-04
	<i>CD163</i>	0.617	8.99E-19
	<i>VSIG4</i>	0.503	4.93E-12
	<i>MS4A4A</i>	0.619	5.79E-19

cells exhibited decreased levels of oxidative stress compared with those in the control group (Figure 4F). The wound healing assay results indicated that enhanced *ST8Sia1* expression impeded tumor cell migration (Figure 4H and I). Moreover, invasion activities (Figure 4J) were significantly curtailed and the apoptosis rates (Figure 4K and Supplementary Figure 3) were obviously increased in the *ST8Sia1*-OE cell group relative to the control group, indicating that *ST8Sia1*-OE can temper the biological functionality of READ cells.

### The impact of *ST8Sia1*-OE on CD8<sup>+</sup> T cell function and tumor cell apoptosis

Subsequently, we explored the effect of *ST8Sia1*-OE on CD8<sup>+</sup> T cell functionality after co-culture with HCT-15 and HCT-116 cells. CD8<sup>+</sup> T cells were successfully purified with high fidelity in the peripheral blood of healthy volunteers (Figure 5A). Following the co-culture of CD8<sup>+</sup> T cells with HCT-15 or HCT-116 cells, we assessed the apoptosis rate in HCT-15 and HCT-116 cell populations in the lower chamber. Our findings illustrated a significant increase in the apoptosis rates of both HCT-15 and HCT-116 cells (Figure 5B and C). Additionally, an observable reduction in the anti-apoptotic molecule Bcl-2 was recorded in *ST8Sia1*-OE cells, whereas the expression of pro-apoptotic molecules Bax, Cleaved caspase 3, and PARP1 was elevated in *ST8Sia1*-OE cells (Figure 5D and E). Then, we assessed the expression levels of Granzyme B and perforin in CD8<sup>+</sup> T cells in the upper chamber. Notably, Granzyme B levels were increased in CD8<sup>+</sup> T cells co-cultured with *ST8Sia1*-OE cells compared to the control group (Figure 5F and G). Similarly, an increase in perforin levels was noted in *ST8Sia1*-OE cells relative to the control group (Figure 5H and I). The expression of IFN-γ and some damage-associated molecular pattern (DAMPs) molecules (HSP, HMGB-1, IL-1α, CRT) was increased in CD8<sup>+</sup> T cells co-cultured with *ST8Sia1*-OE cells compared to the control group (Figure 5J–M).

### *ST8Sia1* interacts with TGF-β1 in HCT-15 cell

To elucidate the impact of *ST8Sia1* on the onset and progression of READ, we stratified the READ data into two distinct cohorts, the *ST8Sia1* high-expression group and the *ST8Sia1* low-expression group, based on the median value of *ST8Sia1* expression. Employing GSEA, we found that the *ST8Sia1* high-expression group predominantly enriched the TGF-β signaling pathway (Figure 6A). Both the protein and mRNA expression levels of TGF-β1 were significantly diminished in the tumor tissues harvested from patients with READ (Figure 6B and C). Subsequently, we engineered elevated TGF-β1 expression in *ST8Sia1*-OE HCT-15 cells to delineate the functional role of TGF-β1 (Figure 6D). Nevertheless, the content of TGF-β1 remained unchanged in different cell culture media, implying that the secretion of TGF-β1 was unaffected by the overexpression of *ST8Sia1* in HCT-15 cells (Supplementary Figure 4). Moreover, immunoprecipitation assays revealed an interaction between *ST8Sia1* and TGF-β1 in HCT15 cells (Figure 6E and F).

**Figure 3.** The ST8Sia1 gene may predict the immunotherapy response of READ. Correlation analysis between ST8Sia1 mRNA expression levels and StromalScore (a), ImmuneScore (B), EstimateScore (C), and TumorPurity (D) in READ. The data was obtained using the “estimate” package in the R environment. (E) The correlation matrix of ST8Sia1 and inflammatory-related metagenes. The correlation coefficients were demonstrated as the proportion of the pie charts, and the specific correlation coefficients were shown on the left. The red parts represented a positive correlation, and the green parts represented a negative correlation. (F) Spearman correlation of ST8Sia1 with ICPs. The width of the band represented the R-value. The color of the band represented the P-value. P-values of  $<0.05$  were considered statistically significant, \*\*\*\* $p < 0.0001$ .

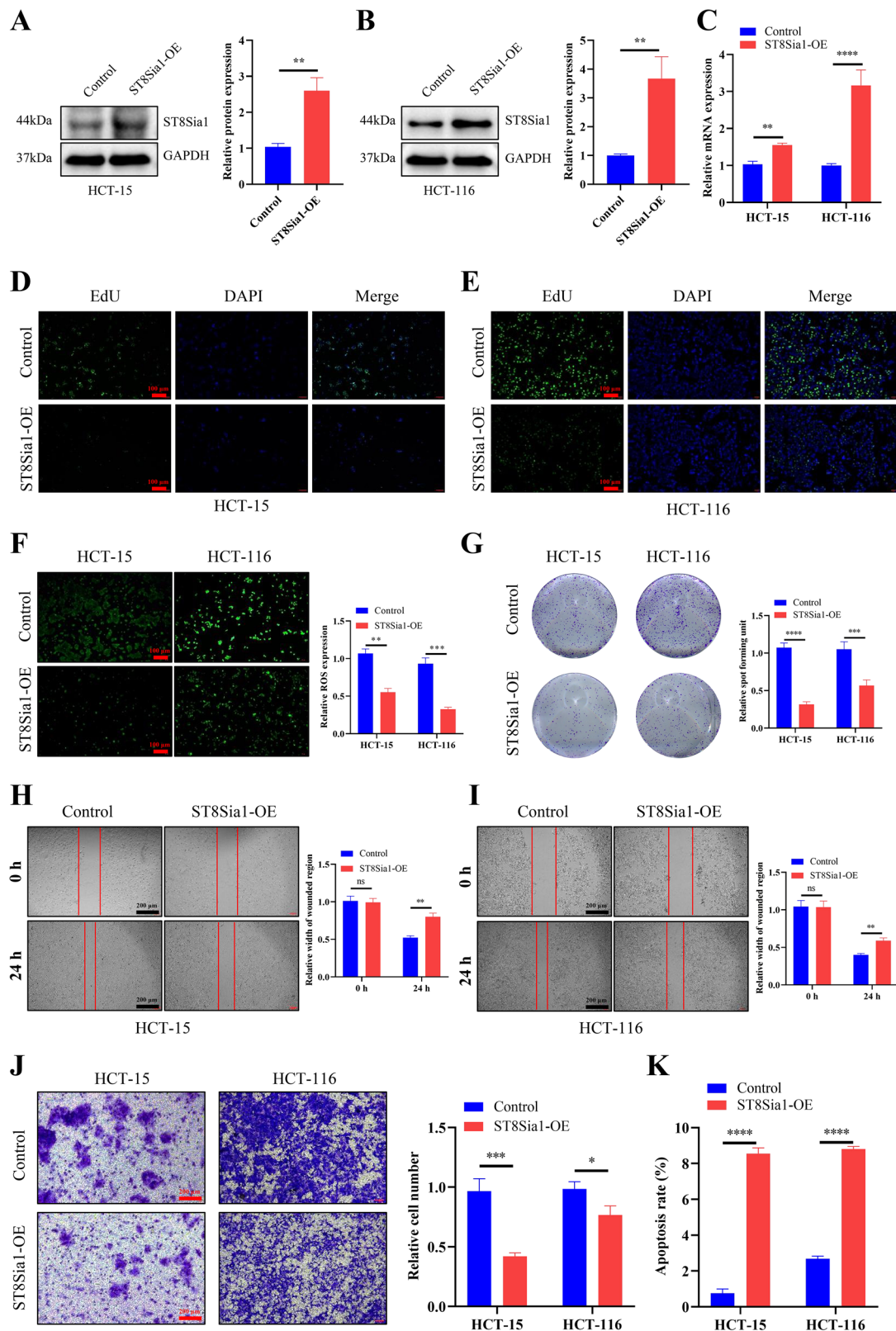


**Figure 4.** ST8Sia1 overexpression inhibited the biological function of READ cells. The protein expression of ST8Sia1 between the ST8Sia1-OE group and control group in HCT-15 cell (A) and HCT-116 cell (B). (C) The mRNA level of ST8Sia1 in the ST8Sia1-OE group and the control group in HCT-15 and HCT-116 cell. EdU assays to detect cell proliferation in HCT-15 (D) and HCT-116 (E) overexpressed with ST8Sia1, Scale bars = 100µm. (F) ROS assay in HCT-15 and HCT-116 overexpressed with ST8Sia1, Scale bars = 100µm. (G) Colony forming assay to detect cell proliferation in HCT-15 and HCT-116 overexpressed with ST8Sia1. Wound healing assays to detect cell migration in HCT-15 (H) and HCT-116 (I) cells overexpressed with ST8Sia1, Scale bars = 200µm. (J) Represented results of the transwell of HCT-15 and HCT-116 cells overexpressed with ST8Sia1, Scale bars = 200µm. (K) The rate of apoptosis between the control group and ST8Sia1-OE group in HCT-15 and HCT-116 cells. \* $p < 0.05$ , \*\* $p < 0.01$ , \*\*\* $p < 0.001$ , and \*\*\*\* $p < 0.0001$ . ns: no statistical significance.

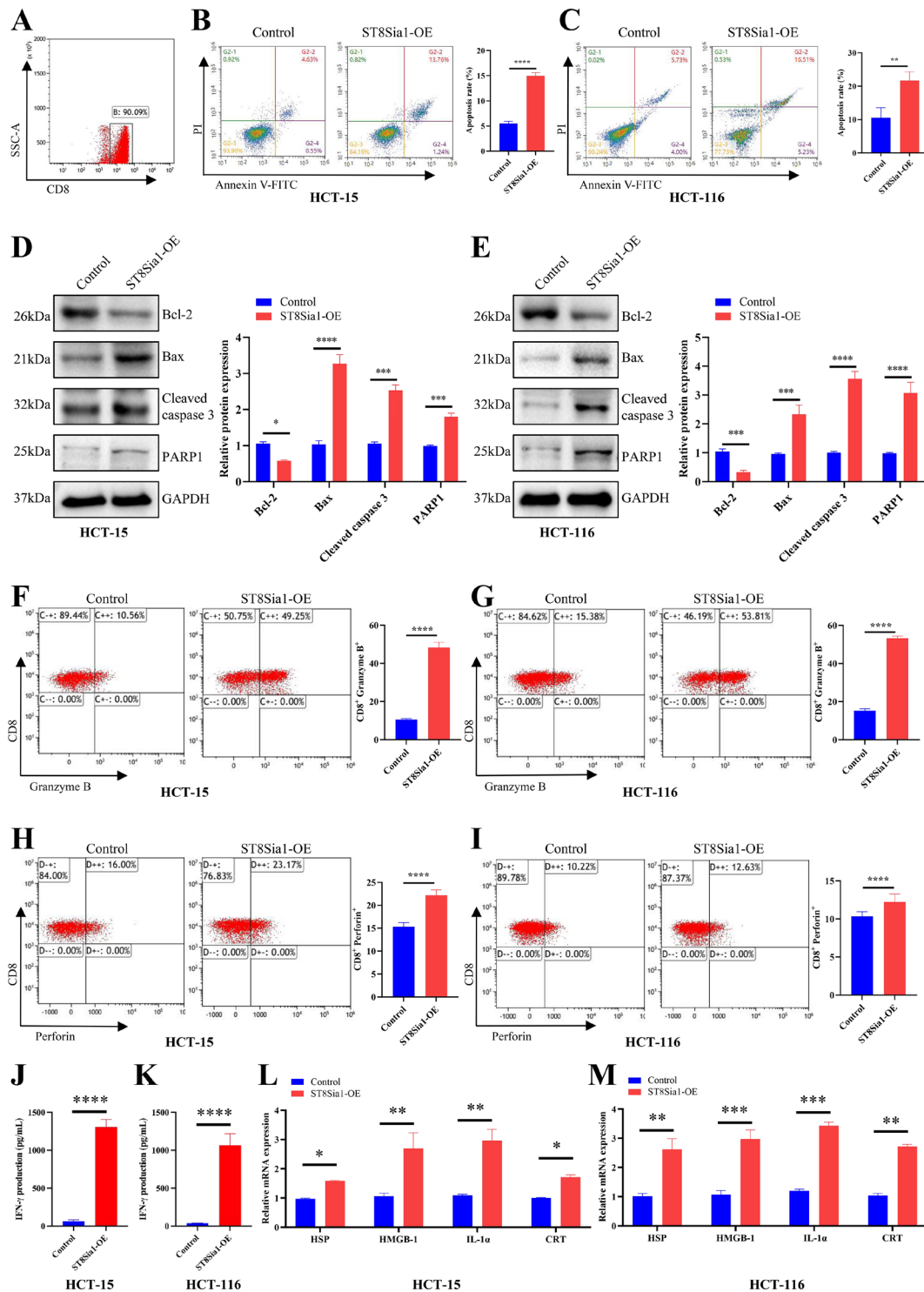


**Figure 5.** The impact of ST8Sia1 overexpression on CD8<sup>+</sup> T cell function and tumor cell apoptosis. (A) The CD8<sup>+</sup> T cells were selected by magnetic beads. (B) Typical flow images of HCT-15 cell apoptosis in each group after co-cultures of CD8<sup>+</sup> T and HCT-15 cells (ST8Sia1-OE and control groups). (C) Typical flow images of HCT-116 cell apoptosis in each group after co-cultures of CD8<sup>+</sup> T and HCT-116 cells (ST8Sia1-OE and control groups). The protein expression of Bcl-2, Bax, Cleaved caspase 3, and PARP1 in HCT-15 cell (D) and HCT-116 cell (E). Typical flow images of Granzyme B expression for each group of CD8<sup>+</sup> T cells co-cultured with HCT-15 cells (ST8Sia1-OE and control groups) (F) and HCT-116 (ST8Sia1-OE and control groups) (G). Typical flow images of perforin expression for each group of CD8<sup>+</sup> T cells co-cultured with HCT-15 cells (ST8Sia1-OE and control groups) (H) and HCT-116 (ST8Sia1-OE and control groups) (I). The level of IFN- $\gamma$  for each group of CD8<sup>+</sup> T cells co-cultured with HCT-15 cells (ST8Sia1-OE and control groups) (J) and HCT-116 (ST8Sia1-OE and control groups) (K). The mRNA expression of HSP, HMGB-1, IL-1 $\alpha$ , CRT in each group of CD8<sup>+</sup> T cells co-cultured with HCT-15 cells (ST8Sia1-OE and control groups) (L) and HCT-116 (ST8Sia1-OE and control groups) (M). \* $p < 0.05$ , \*\* $p < 0.01$ , \*\*\* $p < 0.001$ , and \*\*\*\* $p < 0.0001$ .



### ST8Sia1-OE inhibited the biological function of READ cells by TGF- $\beta$ 1

Subsequently, we investigated whether ST8Sia1 mitigated the onset and progression of READ by modulating TGF- $\beta$ 1. Colony forming assays revealed that TGF- $\beta$ 1 knockdown augmented tumor cell proliferation relative to that in the ST8Sia1-OE group (Figure 7A). Invasive capabilities were significantly higher in the ST8Sia1-OE-shTGF- $\beta$ 1 cohort than in the ST8Sia1-OE group (Figure 7B). The wound healing assay outcomes indicated that TGF- $\beta$ 1 downregulation enhanced tumor

cell migration (Figure 7C). Upon evaluating apoptosis in HCT-15 cells, we observed a significant reduction in the apoptosis rate in the ST8Sia1-OE-shTGF- $\beta$ 1 group compared to the ST8Sia1-OE group (Figure 7D). Moreover, the anti-apoptotic molecule Bcl-2 exhibited elevated expression in ST8Sia1-OE-shTGF- $\beta$ 1 cells, whereas the expression of pro-apoptotic molecules Bax, Cleaved caspase 3, and PARP was attenuated in ST8Sia1-OE-shTGF- $\beta$ 1 cells (Figure 7E).

Additionally, to delineate the impact of ST8Sia1 on the *in vivo* development of READ, we extended our investigation by inoculating athymic male nude mice

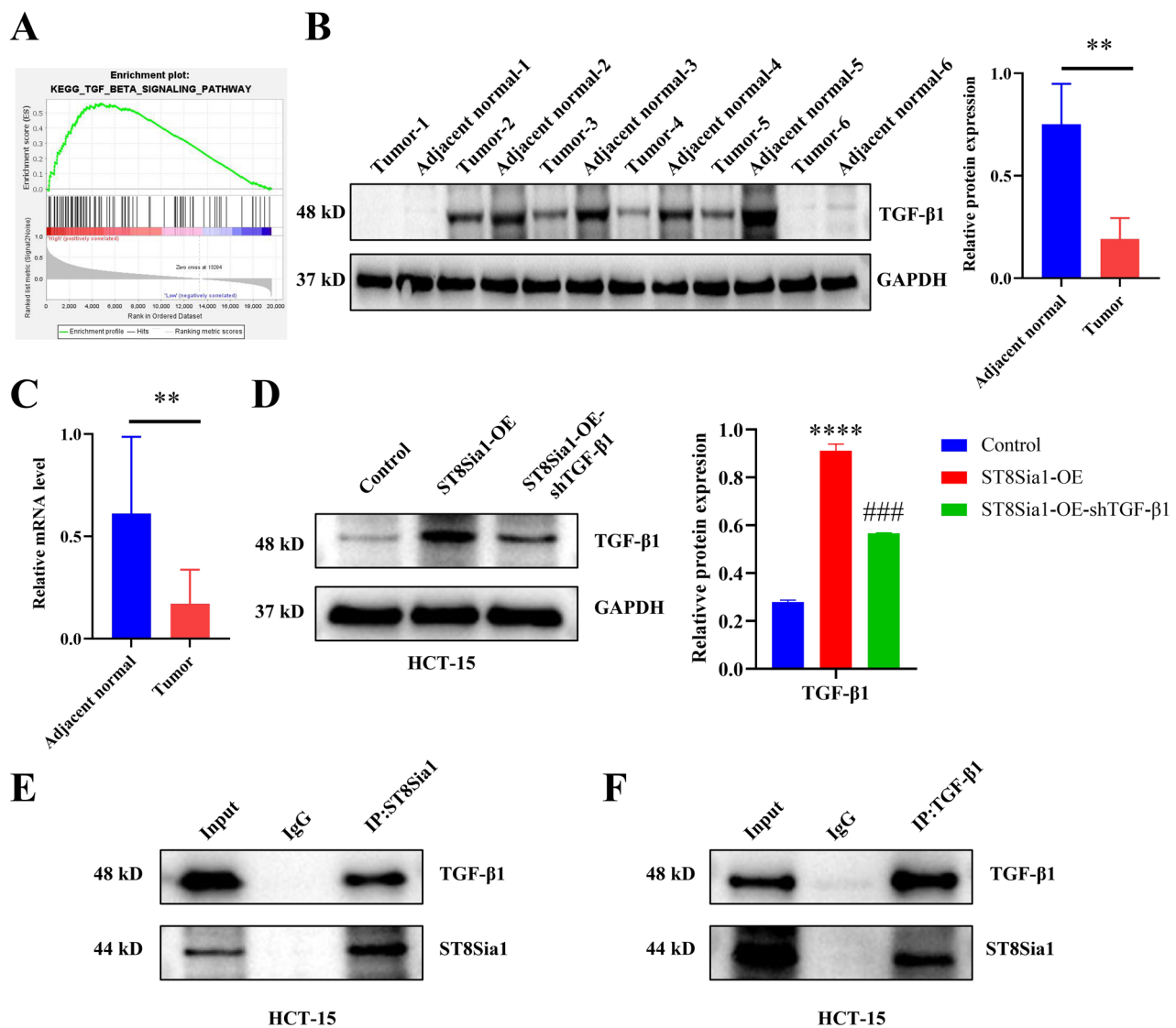


**Figure 6.** ST8Sia1 interacts with TGF- $\beta$ 1 in HCT-15 cell. (A) GSEA plot presentation of significant gene set indicative of the development of a typical TGF- $\beta$  signaling pathway. The TGF- $\beta$ 1 levels were detected in tumor tissues and adjacent normal tissues of patients with READ by WB (B), and RT-qPCR (C) ( $n=6$ ). GAPDH served as a control. (D) The protein expression of TGF- $\beta$ 1 between the control group, ST8Sia1-OE group and ST8Sia1-OE-shTGF- $\beta$ 1 in HCT-15 cell. Immunoprecipitation (IP) followed by immunoblot assay with the whole lysates of HCT-15 cells. Antibodies including IgG and anti-ST8Sia1 were used for IP, with ST8Sia1 and TGF- $\beta$ 1 in both IP products and inputs analyzed (E), antibodies including IgG and anti-TGF- $\beta$ 1 were used for IP, with ST8Sia1 and TGF- $\beta$ 1 in both IP products and inputs analyzed (F). \*\* $p<0.01$  and \*\*\*\* $p<0.0001$ , compared to control group. ### $p<0.01$ , compared to ST8Sia1-OE group.

**Figure 7.** ST8Sia1-OE inhibited the biological function of READ cells by TGF- $\beta$ 1 *in vitro*. (A) Colony forming assay to detect cell proliferation in different group. (B) Represented results of the transwell in different group. Scale bars = 200  $\mu$ m. (C) Wound healing assays to detect cell migration in different group, Scale bars = 200  $\mu$ m. (D) Typical flow images of HCT-116 cell apoptosis in each group. (E) The protein expression of Bcl-2, Bax, Cleaved caspase 3, and PARP1 in HCT-15 cell. \*\*\*\* $p$  < 0.0001, compared to control group. \* $p$  < 0.05, \*\* $p$  < 0.01, \*\*\* $p$  < 0.001 and \*\*\*\* $p$  < 0.0001, compared to ST8Sia1-OE group.

with Control, ST8Sia1-OE, and ST8Sia1-OE-shTGF- $\beta$ 1 HCT15 cells. Remarkably, mice injected with ST8Sia1-OE HCT15 cells exhibited significantly reduced tumor volumes and weights compared to those injected with Control HCT15 cells. However, this phenomenon was reversed by TGF- $\beta$ 1 knockdown (Figure 8A–C). Consistent with these findings, immunohistochemical analyses revealed that the expression levels of ST8Sia1, TGF- $\beta$ 1, Bax, Caspase 3, and Caspase 9 in the tumor tissues of nude mice were significantly diminished in the ST8Sia1-OE-shTGF- $\beta$ 1 group relative to the ST8Sia1-OE group. Conversely, the expression level of Bcl-2 was significantly elevated in the ST8Sia1-OE-shTGF- $\beta$ 1 group (Figure 8D and E). Collectively, these findings underscore the role of TGF- $\beta$ 1 in mediating the inhibitory effects of ST8Sia1-OE on READ onset and progression.

## Discussion

READ combined with colon adenocarcinoma ranks third in the incidence of all tumor cases, and this rate is increasing [27]. The correlation between abnormal glycosylation and the occurrence of READ has been previously reported. The expression of ST6Gal1, which is a primary transferase, has increased and may mediate chemoradiotherapy resistance in READ by inhibiting apoptosis following chemoradiotherapy [28]. The  $\alpha$ 1,6-fucosyltransferase level is increased during the malignant transformation of COAD [29]. Downregulating the expression of Fut5 and Fut6, which are overexpressed in COAD tissues, can halt the invasion and angiogenesis of COAD cells [30]. ST3Gal2 knockdown decreases the tumoral characteristics of COAD cells [31]. The expression of ST3Gal5 is increased in READ tissues and may be involved in rectal carcinogenesis, although the detailed mechanism is unknown [32]. We first authenticated ST8Sias expression in TCGA, GEO, and TIMER 2.0, and revealed their downregulation in the mRNA levels in READ tissues versus normal tissues. ST8Sia2 downregulation results in poor READ prognosis. Univariate and multivariate Cox regression analyses further verified that ST8Sia2 may serve as an independent prognostic factor for OS in patients with READ. Generally, ST8Sia1 is considered to be a “tumor suppressor gene” in READ. Finally, we found that ST8Sia1-OE inhibited tumor cell proliferation, migration, and invasion. The expression of Granzyme B and Perforin on CD8<sup>+</sup> T cells significantly increased, indicating a significant enhancement in tumor-killing function, while the apoptosis rate of tumor cells significantly increased after co-culturing CD8<sup>+</sup> T cells with upregulated ST8Sia1 in HCT-15 and HCT-116 cells. Finally, the presence of TGF- $\beta$ 1 was crucial in restraining the

incidence and progression of READ both *in vivo* and *in vitro* in the context of ST8Sia1-OE (Figure 9).

Our observations indicate increased recruitment of CD4<sup>+</sup> and CD8<sup>+</sup> T cells in the healthy rectal tissues adjacent to tumors in READ patients compared to the tumor tissues themselves. This can be explained by the immune evasion mechanisms that tumors, including READ, commonly employ. These tactics include expressing immune checkpoint molecules such as PD-L1, secreting immunosuppressive cytokines like TGF- $\beta$  and IL-10, and promoting regulatory T cells (Tregs), all of which suppress the activity of cytotoxic T lymphocytes (CTLs) within the tumor microenvironment (TME) [33]. Moreover, the extracellular matrix (ECM) in tumor tissues tends to be denser and more cross-linked than in normal tissues, posing a physical barrier to immune cell infiltration. The TME is often characterized by hypoxia, acidity, and nutrient depletion, further deterring T cell functionality [34, 35]. In contrast, the tumor-adjacent healthy tissues likely preserve functional antigen-presenting cells (APCs) such as dendritic cells, which effectively present tumor antigens to T cells. This may explain the higher T cell recruitment and activation in these regions, supported by lower levels of immunosuppressive factors relative to the TME [36]. Chemokine and chemokine receptor expression differences between tumor and adjacent healthy tissues also influence T cell migration. For example, the presence of CXCL10 and CCL5 in non-tumor tissues attracts CXCR3<sup>+</sup> and CCR5<sup>+</sup> T cells, respectively [37]. Past research has noted variability in effector, memory, and naïve T cell subset proportions within tumor versus adjacent normal tissues, with memory T cells demonstrating preference for non-tumorous tissues due to their superior tissue-residency capabilities [38]. To thoroughly understand the differential recruitment in READ, examining the chemokine-chemokine receptor profiles, ECM characteristics, APC presence, and tumor cell immune evasion strategies in both tissue types is crucial. Additionally, assessing the functionality of CD4<sup>+</sup> and CD8<sup>+</sup> T cells in these diverse contexts would provide deeper insight into their potential roles in anti-tumor responses or suppressive activities.

The activation of CD8<sup>+</sup> T cells generally involves T-cell receptor (TCR) interaction with peptide-MHC class I complexes on the target cells, leading to T-cell activation, proliferation, and cytotoxic function. In the typical scenario involving direct cell contact, this interaction is crucial for the specificity and restriction of the CD8<sup>+</sup> T cell response. However, in a transwell system, this direct interaction is impeded, prompting an investigation into how activation occurs in this setting. Several studies have shown that apart from direct

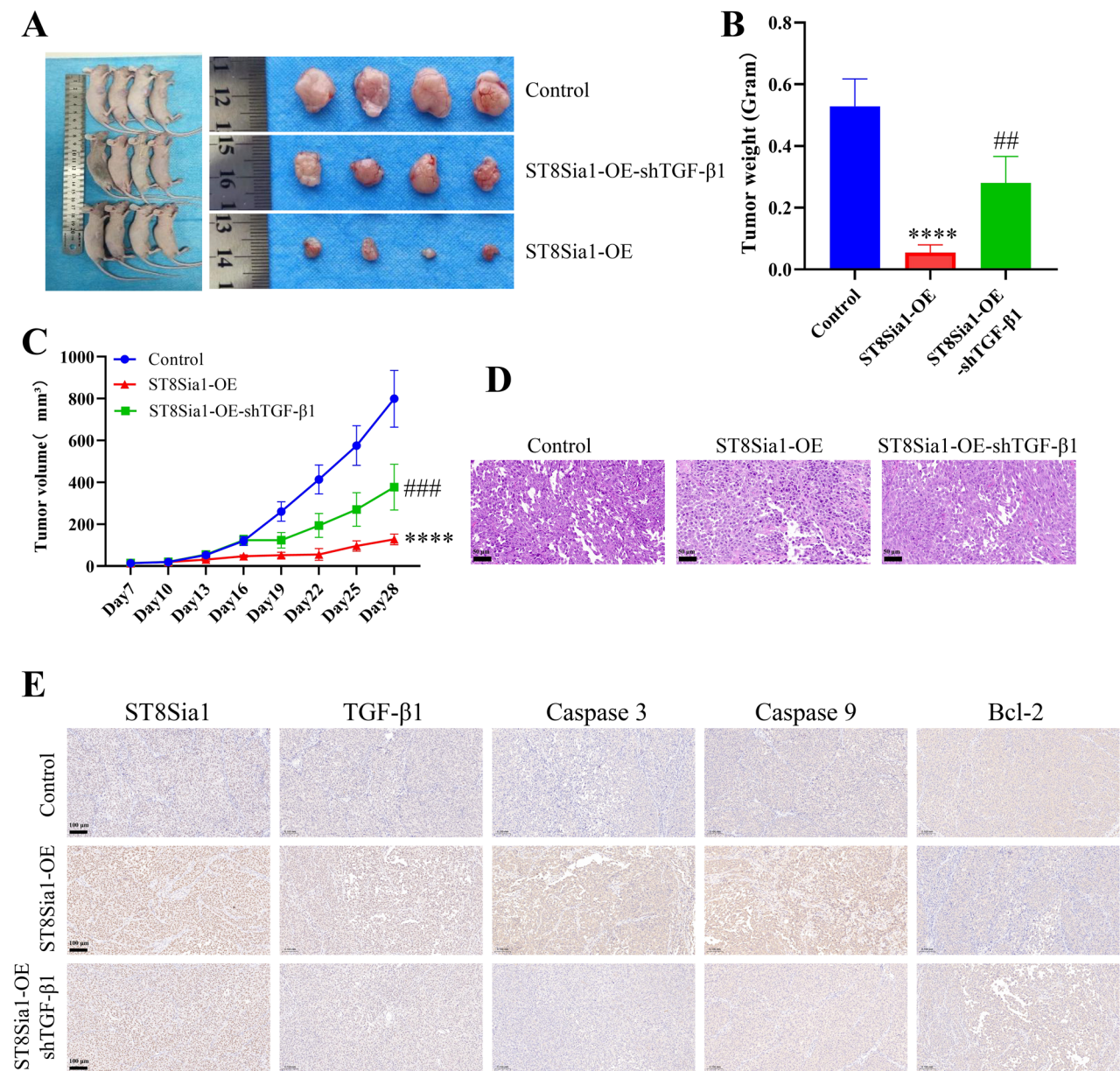


**Figure 8.** ST8Sia1-OE inhibited the biological function of READ cells by TGF-β1 *in vivo*. (A) Control, ST8Sia1-OE and ST8Sia1-OE-shTGF-β1 HCT cells were injected into nude mice to detect tumor formation *in vivo*. (B) The tumor weight of Control, ST8Sia1-OE and ST8Sia1-OE-shTGF-β1 group. (C) Tumor volume in nude mice was calculated using the formula:  $1/2 \times (\text{length} \times \text{width}^2)$  ( $n=4$ ). (D) The images of H&E staining results for normal and tumor patient tissues ( $n=3$ ), Scale bars = 50 μm. (E) The images of immunohistochemical staining results of different proteins in normal and tumor patient tissues ( $n=3$ ), Scale bars = 100 μm. \*\*\*\* $p < 0.0001$ , compared to Control group. \*\* $p < 0.01$  and \*\*\* $p < 0.001$ , compared to ST8Sia1-OE group.

cell-cell interaction, CD8<sup>+</sup> T cells can also be activated by tumor-derived soluble factors. These factors, often cytokines and chemokines, can stimulate T cells in a manner that does not strictly require TCR-MHC class I interaction. This type of activation is sometimes referred to as "bystander activation" where T cells can become activated without specific antigen recognition through their TCR. For instance, interleukin-15 (IL-15) is a cytokine known to enhance the cytotoxicity of CD8<sup>+</sup> T cells by increasing the production of granzyme B and perforin independently of TCR specificity [39].

IL-15 can be produced by various tumor cells and might act on nearby CD8<sup>+</sup> T cells, leading them to exhibit cytotoxic behaviors even without specific antigen engagement. Furthermore, other soluble factors such as IL-12, IL-18, and IFNs have also been reported to activate CD8<sup>+</sup> T cells and increase their cytolytic activity [40]. These cytokines may be part of the milieu produced by tumor cells (including HCT cells) and could contribute to the activation observed in the transwell systems. Regarding the specificity and restriction typically required for CD8<sup>+</sup> T cell activation, these



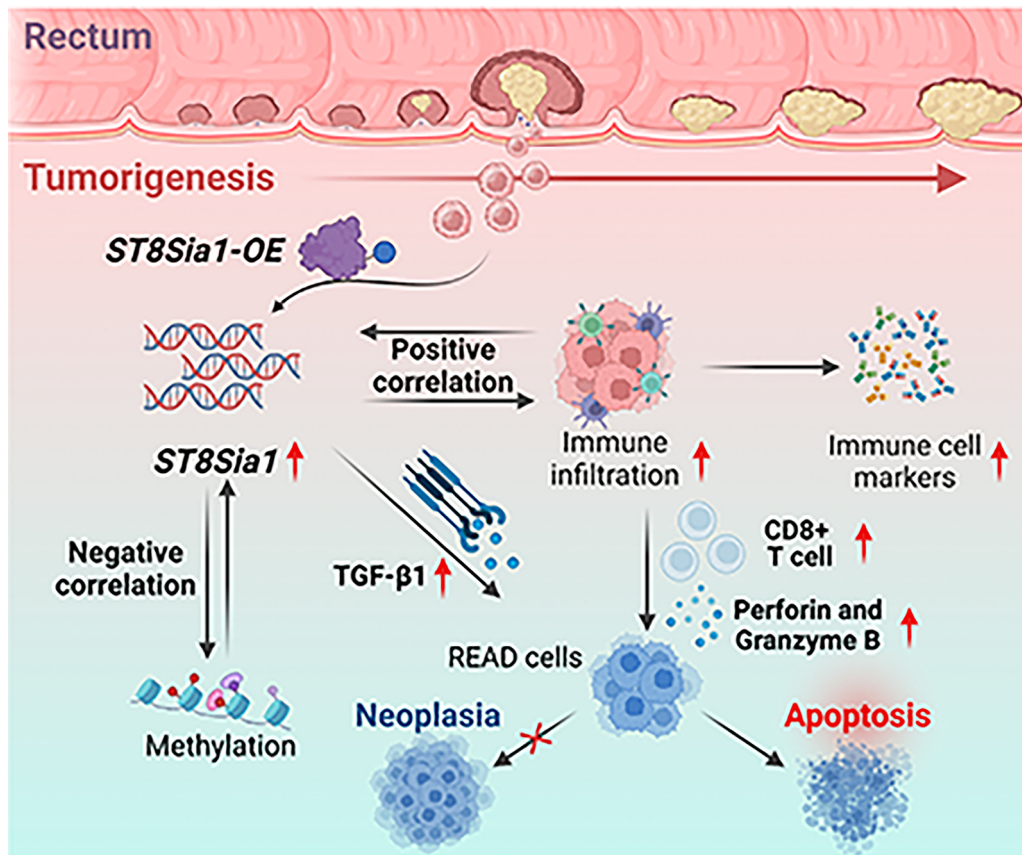


**Figure 9.** The mechanism of overexpressed ST8Sia1 inhibits tumor progression and promotes the tumoricidal effects of CD8<sup>+</sup> T cells in rectal adenocarcinoma (READ) is through TGF- $\beta$ 1 signaling. In READ tissues compared to normal tissues, there was a down-regulation in the mRNA levels of ST8Sia1. Tumor cell proliferation, migration, and invasion were inhibited by ST8Sia1 over-expression (ST8Sia1-OE). The increase in the expression of granzyme B and perforin on CD8<sup>+</sup> T cells indicates a significant improvement in their tumor-killing function, while the apoptosis rate of tumor cells also significantly increases when CD8<sup>+</sup> T cells are co-cultured with HCT-15 or HCT-116 cells that have up-regulated ST8Sia1. The presence of TGF- $\beta$ 1 is crucial in limiting the occurrence and advancement of READ both *in vivo* and *in vitro* in the context of ST8Sia1-OE.

processes in the context of cytokine-driven activation can be less strict. While TCR specificity and MHC Class I restriction are central to traditional antigen-specific T-cell responses, the actions of these cytokines suggest parallel pathways that can coax CD8<sup>+</sup> T cells into a functional state. These alternative activation routes are particularly crucial in tumor immunity, where tumor cells might evade immune surveillance by downregulating MHC molecules or altering antigen processing machinery.

Aberrant DNA methylation changes, including both DNA hypermethylation and hypomethylation events, are closely associated with cancer occurrence, and disruption of cancer is a characteristic of DNA methylation [41, 42]. The upregulated N-acetylgalactosaminyltransferase 2/14 (GalNT2/14) and their methylation expression levels were reversed, and lung adenocarcinoma patients with upregulated GalNT2/14 expression had poor overall survival (OS) [43]. Additionally, hypermethylation levels of GAL, GALR1, and GALR2 exhibited the strongest association with poor survival in patients with HNSC [44]. Our

study revealed that the DNA methylation levels of ST8Sia1 were upregulated in READ and negatively correlated with downregulated ST8Sia1 expression. Furthermore, the hypermethylation status of ST8Sia1 may serve as an important biomarker for predicting the development and progression of READ.

The status of tumor-infiltrating lymphocytes regulates tumorigenesis and tumor progression [45, 46]. However, whether ST8Sia1 regulates tumor-infiltrating immune cells in READ remains unclear. ST8Sia1 was positively related with the StromalScore, ImmuneScore, and ESTIMATEScore in READ. This indicates that ST8Sia1 regulates the TME, which explains the immunosuppressive state of low ST8Sia1 expression. We examined the link between ST8Sia1 and immune-related pathways by GSVA and revealed that ST8Sia1 expression was positively correlated with the immune response, including the T/B cell-related immune response. The expression of ST8Sia1 may regulate the immune response in READ, indicating its potential of ST8Sia1 as a READ immunotherapy target. These results strongly

indicated the potential of ST8Sia1 as an anticancer immunotherapy target.

Through GSEA, we found that the high-expression group of ST8Sia1 was mainly enriched in the TGF- $\beta$  signaling pathway. Furthermore, subsequent studies have shown that the expression levels of TGF- $\beta$ 1 protein and mRNA were significantly decreased in the tumor tissues of patients with READ. Immunoprecipitation experiments revealed an interaction between ST8Sia1 and TGF- $\beta$ 1 in HCT-15 cells. Moreover, in further investigations, we found that overexpression of ST8Sia1 in cells with knockdown of TGF- $\beta$ 1, its inhibitory effect on tumor cells. The role of TGF- $\beta$  and its signaling pathway molecules has been studied in various cancers, including CRC. It is an effective regulator of cell adhesion, movement, extracellular matrix production, angiogenesis and immunosuppression [47, 48]. High TGF- $\beta$  expression is often associated with late disease, tumor recurrence, and reduced patient survival. Several studies have shown that increased TGF- $\beta$  expression is associated with reduced disease progression and survival in CRC patients [49]. TGF- $\beta$  promotes fibrosis of the tumoral stroma; thus, immune cell infiltration is inhibited [50]. However, low TGF- $\beta$ 1 protein expression is associated with an adverse prognosis in patients with stage III rectal cancer [51]. In our study, we found that ST8Sia1 significantly promoted TGF- $\beta$ 1 expression. Knockdown of TGF- $\beta$ 1 can prevent the overexpression of ST8Sia1 and suppress READ, suggesting that TGF- $\beta$ 1 is ST8Sia1 necessary to suppress READ. TGF $\beta$ 1 is known for its dual role in the immune context, where it generally acts as an immunosuppressive molecule but can also promote immunogenic responses under certain conditions [52]. The interaction between ST8Sia1 and TGF $\beta$ 1 suggests a novel axis through which ST8Sia1 may modify the tumor microenvironment to favor an immune-responsive condition *via* modulating TGF $\beta$ 1 dynamics, consequently enhancing effector functions of CD8<sup>+</sup> T cells. Given these results, we hypothesize that the overexpression of ST8Sia1 in tumor cells may lead to an altered TGF $\beta$ 1 profile, which in turn modulates the cytotoxic activity of neighboring CD8<sup>+</sup> T cells. This modulation likely tilts the balance from an immunosuppressive to a more immunogenic milieu, promoting the release of factors like perforin and granzyme B that are crucial for CD8<sup>+</sup> T cell-mediated cytotoxicity. Further investigations should focus on detailed pathways linking TGF $\beta$ 1 and ST8Sia1 interaction to changes in the tumor microenvironment, and how these alterations influence the priming and activation of naive or unspecific CD8<sup>+</sup> T cells. Comprehensive studies could include the use of cytokine profiling, advanced imaging

technologies, and functional assays to map the regulatory networks influenced by ST8Sia1 and TGF $\beta$ 1 in various cancer models. In conclusion, our data propose a novel mechanistic insight into how ST8Sia1 overexpression in tumor cells can potentiate the cytotoxic activity of CD8<sup>+</sup> T cells through a TGF $\beta$ 1-dependent pathway. This underscores the potential of ST8Sia1 as a therapeutic target in cancer immunotherapy strategies aimed at enhancing CD8<sup>+</sup> T cell functions.

## Conclusion

This study revealed downregulated expression levels of ST8Sia1 in READ tissues versus normal tissues, which were negatively correlated with methylation levels. In addition, we revealed the underlying immune regulatory mechanisms of ST8Sia1 in READ. Ultimately, ST8Sia1-OE can help restore immune cell function and provide a clinical approach for the combined cellular immunotherapy of READ. Overall, ST8Sia1 may be a novel diagnostic marker and immune cell infiltration predictor in patients with READ.

## Consent for publication

The authors are accountable for all aspects of the work, ensuring that questions related to the accuracy or integrity of any part of the work are appropriately investigated and resolved.

## Authors contributions

Conceptualization: X. X and L. H; Methodology: L.H, C. Z, and Y. Y; Software: C. Z; Validation: Y. W; Formal analysis: Y. W and Y. Y; Investigation: Y. W; Resources: Y. W and Y. Y; Data curation: C. Z and Y. Y; Writing - original draft: C. Z and Y. W; Writing - review & editing: L.H, Y. P, and X. X; Visualization: Y. P and Y. W; Supervision: Y. P. All authors critically reviewed the article and approved the final manuscript.

## Disclosure statement

No potential conflict of interest was reported by the author(s).

## Funding

The author(s) reported there is no funding associated with the work featured in this article.

## ORCID

Leilei Hao  <http://orcid.org/0009-0002-7276-3261>

## Data availability statement

The data that support the findings of this study are available from the corresponding author, L.H, upon reasonable request. The RNA-seq data of human READ tissues were derived from the following resources available in the public domain: GEO database (number GSE87211) at <https://www.ncbi.nlm.nih.gov/geo/query/acc.cgi?acc=GSE87211> and TCGA database (TCGA-READ) at <https://www.cancer.gov/ccg/research/genome-sequencing/tcga>.

## References

- [1] He F, Ju H-Q, Ding Y, et al. Association between adjuvant chemotherapy and survival in patients with rectal cancer and pathological complete response after neoadjuvant chemoradiotherapy and resection. *Br J Cancer*. 2020;123(8):1244–1252. doi: [10.1038/s41416-020-0989-1](https://doi.org/10.1038/s41416-020-0989-1).
- [2] Gaertner WB, Kwaan MR, Madoff RD, et al. Rectal cancer: an evidence-based update for primary care providers. *World J Gastroenterol*. 2015;21(25):7659–7671. doi: [10.3748/wjg.v21.i25.7659](https://doi.org/10.3748/wjg.v21.i25.7659).
- [3] Deng Y. Rectal cancer in Asian vs. Western countries: why the variation in incidence? *Curr Treat Options Oncol*. 2017;18(10):64. doi: [10.1007/s11864-017-0500-2](https://doi.org/10.1007/s11864-017-0500-2).
- [4] Chen W, Zheng R, Baade PD, et al. Cancer statistics in China, 2015. *CA Cancer J Clin*. 2016;66(2):115–132. doi: [10.3322/caac.21338](https://doi.org/10.3322/caac.21338).
- [5] Benson AB, Venook AP, Al-Hawary MM, et al. Rectal Cancer, Version 2.2018, NCCN clinical practice guidelines in oncology. *J Natl Compr Canc Netw*. 2018;16(7):874–901. doi: [10.6004/jnccn.2018.0061](https://doi.org/10.6004/jnccn.2018.0061).
- [6] Canda AE, Terzi C, Gorken IB, et al. Effects of preoperative chemoradiotherapy on anal sphincter functions and quality of life in rectal cancer patients. *Int J Colorectal Dis*. 2010;25(2):197–204. doi: [10.1007/s00384-009-0807-y](https://doi.org/10.1007/s00384-009-0807-y).
- [7] Fuster MM, Esko JD. The sweet and sour of cancer: glycans as novel therapeutic targets. *Nat Rev Cancer*. 2005;5(7):526–542. doi: [10.1038/nrc1649](https://doi.org/10.1038/nrc1649).
- [8] Andergassen U, Liesche F, Kölbl AC, et al. Glycosyltransferases as markers for early tumorigenesis. *Biomed Res Int*. 2015;2015:792672–792611. doi: [10.1155/2015/792672](https://doi.org/10.1155/2015/792672).
- [9] Dobie C, Skropeta D. Insights into the role of sialylation in cancer progression and metastasis. *Br J Cancer*. 2021;124(1):76–90. doi: [10.1038/s41416-020-01126-7](https://doi.org/10.1038/s41416-020-01126-7).
- [10] Lin W-D, Fan T-C, Hung J-T, et al. Sialylation of CD55 by ST3GAL1 facilitates immune evasion in cancer. *Cancer Immunol Res*. 2021;9(1):113–122. doi: [10.1158/2326-6066.CIR-20-0203](https://doi.org/10.1158/2326-6066.CIR-20-0203).
- [11] Pearce OM, Läubli H. Sialic acids in cancer biology and immunity. *Glycobiology*. 2016;26(2):111–128. doi: [10.1093/glycob/cwv097](https://doi.org/10.1093/glycob/cwv097).
- [12] Yang Y, Murai R, Takahashi Y, et al. Comparative studies of polysialic acids derived from five different vertebrate brains. *Int J Mol Sci*. 2020;21(22):8593. doi: [10.3390/ijms21228593](https://doi.org/10.3390/ijms21228593).
- [13] Ramos RI, Bustos MA, Wu J, et al. Upregulation of cell surface GD3 ganglioside phenotype is associated with human melanoma brain metastasis. *Mol Oncol*. 2020;14(8):1760–1778. doi: [10.1002/1878-0261.12702](https://doi.org/10.1002/1878-0261.12702).
- [14] Oblinger JL, Pearl DK, Boardman CL, et al. Diagnostic and prognostic value of glycosyltransferase mRNA in glioblastoma multiforme patients. *Neuropathol Appl Neurobiol*. 2006;32(4):410–418. doi: [10.1111/j.1365-2990.2006.00742.x](https://doi.org/10.1111/j.1365-2990.2006.00742.x).
- [15] Ruckhäberle E, Rody A, Engels K, et al. Microarray analysis of altered sphingolipid metabolism reveals prognostic significance of sphingosine kinase 1 in breast cancer. *Breast Cancer Res Treat*. 2008;112(1):41–52. doi: [10.1007/s10549-007-9836-9](https://doi.org/10.1007/s10549-007-9836-9).
- [16] Zhao Y, Li Y, Ma H, et al. Withdrawal: modification of sialylation mediates the invasive properties and chemosensitivity of human hepatocellular carcinoma. *Mol Cell Proteomics*. 2019;18(6):1269. doi: [10.1074/mcp.W119.001568](https://doi.org/10.1074/mcp.W119.001568).
- [17] Ma W, Zhao X, Liang L, et al. miR-146a and miR-146b promote proliferation, migration and invasion of follicular thyroid carcinoma via inhibition of ST8SIA4. *Oncotarget*. 2017;8(17):28028–28041. doi: [10.18632/oncotarget.15885](https://doi.org/10.18632/oncotarget.15885).
- [18] Ma X, Dong W, Su Z, et al. Functional roles of sialylation in breast cancer progression through miR-26a/26b targeting ST8SIA4. *Cell Death Dis*. 2016;7(12):e2561–e2561. doi: [10.1038/cddis.2016.427](https://doi.org/10.1038/cddis.2016.427).
- [19] Ko C-Y, Chu T-H, Hsu C-C, et al. Bioinformatics analyses identify the therapeutic potential of ST8SIA6 for colon cancer. *J Pers Med*. 2022;12(3):401. doi: [10.3390/jpm12030401](https://doi.org/10.3390/jpm12030401).
- [20] Hu Y, Gaedcke J, Emons G, et al. Colorectal cancer susceptibility loci as predictive markers of rectal cancer prognosis after surgery. *Genes Chromosomes Cancer*. 2018;57(3):140–149. doi: [10.1002/gcc.22512](https://doi.org/10.1002/gcc.22512).
- [21] Li T, Fu J, Zeng Z, et al. TIMER2.0 for analysis of tumor-infiltrating immune cells. *Nucleic Acids Res*. 2020;48(W1):W509–W514. doi: [10.1093/nar/gkaa407](https://doi.org/10.1093/nar/gkaa407).
- [22] Chandrashekar DS, Bashel B, Balasubramanya SAH, et al. UALCAN: A portal for facilitating tumor subgroup gene expression and survival analyses. *Neoplasia*. 2017;19(8):649–658. doi: [10.1016/j.neo.2017.05.002](https://doi.org/10.1016/j.neo.2017.05.002).
- [23] Yoshihara K, Shahmoradgoli M, Martínez E, et al. Inferring tumour purity and stromal and immune cell admixture from expression data. *Nat Commun*. 2013;4(1):2612. doi: [10.1038/ncomms3612](https://doi.org/10.1038/ncomms3612).
- [24] Hänzelmann S, Castelo R, Guinney J. GSVA: gene set variation analysis for microarray and RNA-seq data. *BMC Bioinformatics*. 2013;14(1):7. doi: [10.1186/1471-2105-14-7](https://doi.org/10.1186/1471-2105-14-7).
- [25] Sherman BT, Hao M, Qiu J, et al. DAVID: a web server for functional enrichment analysis and functional annotation of gene lists (2021 update). *Nucleic Acids Res*. 2022;50(W1):W216–W221. doi: [10.1093/nar/gkac194](https://doi.org/10.1093/nar/gkac194).
- [26] Huang da W, Sherman BT, Lempicki RA. Systematic and integrative analysis of large gene lists using DAVID bioinformatics resources. *Nat Protoc*. 2009;4(1):44–57. doi: [10.1038/nprot.2008.211](https://doi.org/10.1038/nprot.2008.211).
- [27] Siegel RL, Miller KD, Jemal A. Cancer statistics, 2020. *CA Cancer J Clin*. 2020;70(1):7–30. doi: [10.3322/caac.21590](https://doi.org/10.3322/caac.21590).
- [28] Smithson M, Irwin R, Williams G, et al. Sialyltransferase ST6GAL-1 mediates resistance to chemoradiation in rectal cancer. *J Biol Chem*. 2022;298(3):101594. doi: [10.1016/j.jbc.2022.101594](https://doi.org/10.1016/j.jbc.2022.101594).
- [29] Muñelo-Romay L, Vázquez-Martín C, Villar-Portela S, et al. Expression and enzyme activity of alpha(1,6)fucosyltransferase 1 in human colorectal cancer.

- syltransferase in human colorectal cancer. *Int J Cancer*. 2008;123(3):641–646. doi: [10.1002/ijc.23521](https://doi.org/10.1002/ijc.23521).
- [30] Liang L, Gao C, Li Y, et al. miR-125a-3p/FUT5-FUT6 axis mediates colorectal cancer cell proliferation, migration, invasion and pathological angiogenesis via PI3K-Akt pathway. *Cell Death Dis*. 2017;8(8):e2968. doi: [10.1038/cddis.2017.352](https://doi.org/10.1038/cddis.2017.352).
  - [31] Deschuyter M, Leger DY, Verboom A, et al. ST3GAL2 knock-down decreases tumoral character of colorectal cancer cells *in vitro* and *in vivo*. *Am J Cancer Res*. 2022;12(1):280–302.
  - [32] Choi SY, Jang JH, Kim KR. Analysis of differentially expressed genes in human rectal carcinoma using suppression subtractive hybridization. *Clin Exp Med*. 2011;11(4):219–226. doi: [10.1007/s10238-010-0130-5](https://doi.org/10.1007/s10238-010-0130-5).
  - [33] Sharma P, Allison JP. The future of immune checkpoint therapy. *Science*. 2015;348(6230):56–61. doi: [10.1126/science.aaa8172](https://doi.org/10.1126/science.aaa8172).
  - [34] Chen Z, Han F, Du Y, et al. Hypoxic microenvironment in cancer: molecular mechanisms and therapeutic interventions. *Signal Transduct Target Ther*. 2023;8(1):70. doi: [10.1038/s41392-023-01332-8](https://doi.org/10.1038/s41392-023-01332-8).
  - [35] Maman S, Witz IP. A history of exploring cancer in context. *Nat Rev Cancer*. 2018;18(6):359–376. doi: [10.1038/s41568-018-0006-7](https://doi.org/10.1038/s41568-018-0006-7).
  - [36] Fridman WH, Zitvogel L, Sautès-Fridman C, et al. The immune contexture in cancer prognosis and treatment. *Nat Rev Clin Oncol*. 2017;14(12):717–734. doi: [10.1038/nrclinonc.2017.101](https://doi.org/10.1038/nrclinonc.2017.101).
  - [37] Homey B, Müller A, Zlotnik A. Chemokines: agents for the immunotherapy of cancer? *Nat Rev Immunol*. 2002;2(3):175–184. doi: [10.1038/nri748](https://doi.org/10.1038/nri748).
  - [38] Amsen D, van Gisbergen K, Hombrink P, et al. Tissue-resident memory T cells at the center of immunity to solid tumors. *Nat Immunol*. 2018;19(6):538–546. doi: [10.1038/s41590-018-0114-2](https://doi.org/10.1038/s41590-018-0114-2).
  - [39] Bergamaschi C, Pandit H, Nagy BA, et al. Heterodimeric IL-15 delays tumor growth and promotes intratumoral CTL and dendritic cell accumulation by a cytokine network involving XCL1, IFN- $\gamma$ , CXCL9 and CXCL10. *J Immunother Cancer*. 2020;8(1):e000599. doi: [10.1136/jitc-2020-000599](https://doi.org/10.1136/jitc-2020-000599).
  - [40] Wawrocki S, Druszczyńska M, Kowalewicz-Kulbat M, et al. Interleukin 18 (IL-18) as a target for immune intervention. *Acta Biochim Pol*. 2016;63(1):59–63. doi: [10.18388/abp.2015\\_1153](https://doi.org/10.18388/abp.2015_1153).
  - [41] Dai X, Ren T, Zhang Y, et al. Methylation multiplicity and its clinical values in cancer. *Expert Rev Mol Med*. 2021;23:e2. doi: [10.1017/erm.2021.4](https://doi.org/10.1017/erm.2021.4).
  - [42] Skvortsova K, Stirzaker C, Taberlay P. The DNA methylation landscape in cancer. *Essays Biochem*. 2019;63(6):797–811. doi: [10.1042/EBC20190037](https://doi.org/10.1042/EBC20190037).
  - [43] Kroes RA, Moskal JR. The role of DNA methylation in ST6Gal1 expression in gliomas. *Glycobiology*. 2016;26(12):1271–1283. doi: [10.1093/glycob/cww058](https://doi.org/10.1093/glycob/cww058).
  - [44] Misawa K, Mochizuki D, Endo S, et al. Site-specific methylation patterns of the GAL and GALR1/2 genes in head and neck cancer: potential utility as biomarkers for prognosis. *Mol Carcinog*. 2017;56(3):1107–1116. doi: [10.1002/mc.22577](https://doi.org/10.1002/mc.22577).
  - [45] Xiao Y, Yu D. Tumor microenvironment as a therapeutic target in cancer. *Pharmacol Ther*. 2021;221:107753. doi: [10.1016/j.pharmthera.2020.107753](https://doi.org/10.1016/j.pharmthera.2020.107753).
  - [46] Wu D, Ding Y, Wang T, et al. Significance of tumor-infiltrating immune cells in the prognosis of colon cancer. *Onco Targets Ther*. 2020;13:4581–4589. doi: [10.2147/OTT.S250416](https://doi.org/10.2147/OTT.S250416).
  - [47] Li X, Liu B, Xiao J, et al. Roles of VEGF-C and Smad4 in the lymphangiogenesis, lymphatic metastasis, and prognosis in colon cancer. *J Gastrointest Surg*. 2011;15(11):2001–2010. doi: [10.1007/s11605-011-1627-2](https://doi.org/10.1007/s11605-011-1627-2).
  - [48] Langenskiöld M, Holmdahl L, Falk P, et al. Increased TGF-beta 1 protein expression in patients with advanced colorectal cancer. *J Surg Oncol*. 2008;97(5):409–415. doi: [10.1002/jso.20961](https://doi.org/10.1002/jso.20961).
  - [49] Gulubova M, Manolova I, Ananiev J, et al. Role of TGF-beta1, its receptor TGFbetaRII, and Smad proteins in the progression of colorectal cancer. *Int J Colorectal Dis*. 2010;25(5):591–599. doi: [10.1007/s00384-010-0906-9](https://doi.org/10.1007/s00384-010-0906-9).
  - [50] Monjazeb AM, Schalper KA, Villarroel-Espindola F, et al. Effects of radiation on the tumor microenvironment. *Semin Radiat Oncol*. 2020;30(2):145–157. doi: [10.1016/j.semradonc.2019.12.004](https://doi.org/10.1016/j.semradonc.2019.12.004).
  - [51] Chun H-K, Jung KU, Choi Y-L, et al. Low expression of transforming growth factor beta-1 in cancer tissue predicts a poor prognosis for patients with stage III rectal cancers. *Oncology*. 2014;86(3):159–169. doi: [10.1159/000358064](https://doi.org/10.1159/000358064).
  - [52] Batlle E, Massagué J. Transforming growth factor- $\beta$  signaling in immunity and cancer. *Immunity*. 2019;50(4):924–940. doi: [10.1016/j.immuni.2019.03.024](https://doi.org/10.1016/j.immuni.2019.03.024).